Journal of Process Control 20 (2010) 396–407

Contents lists available at ScienceDirect

Journal of Process Control

journal homepage: www.elsevier.com/locate/jprocont

Optimization-based automatic flatness control in cold tandem rolling

Alberto Bemporad [a], Daniele Bernardini [a], Francesco Alessandro Cuzzola [b,*], Andrea Spinelli [a]

[a] Department of Information Engineering, University of Siena, Italy
[b] Danieli Automation SpA, Italy

ARTICLE INFO

Article history:
Received 1 January 2009
Received in revised form 4 February 2010
Accepted 4 February 2010

Keywords:
Automatic flatness control
Cold tandem rolling mill
Model predictive control

ABSTRACT

For the problem of automatic flatness control (AFC) in cold tandem mills this paper proposes control techniques based on quadratic optimization and delay compensation. Three different strategies are presented and compared: a centralized solution based on a global quadratic programming (QP) problem that decides the commands to all the actuators, and two decentralized solutions where each actuator command is optimized locally. All schemes are based on a global exchange of information about the commands generated at the previous time step at each stand to compensate for the numerous delays present in the mill. Control algorithms are tested in simulation considering a tandem mill with five stands as a benchmark, and results are shown to demonstrate the performance of the proposed schemes.

1. Introduction

Flat cold tandem mills (see [1]) have the purpose of reducing the thickness of flat steel by means of consecutive rolling passes, i.e. through 3–5 housings called rolling stands. This type of process is widely exploited in order to feed a wide variety of industries from food industry to automotive industry. In the recent years, the production of steel (and other metals like copper and aluminium as well) by cold rolling has been subject of research efforts to reach ultra-thin gauges and to increment the production performance together with the quality of the material.

The automation behind this process resorts to complex control technologies and advanced hardware solutions that are often organized in two hierarchical layers. The PLC automation level (Level 1 automation) is in charge of regulating in closed-loop the thickness and the flatness by means of real-time operative systems, whereas the Level 2 automation optimizes the so-called *setup* that defines, in particular, the reduction to be performed by each rolling stand, the prediction of the rolling force applied by each stand, the target flatness to be realized also by an intermediate rolling stand, and, finally, the initial best configuration of the flatness actuators. This calculation is executed offline, i.e. before the beginning of the rolling process, by suitable process computers where complex mathematical models and identification techniques are implemented (see e.g. [2–4]).

The cold tandem rolling can be included as an example of the more general field of sheet and film processing (see the survey [5]). It is necessary to point out that between these processes there are strong differences related not only to the mechanical and sensors solutions, but also to the characteristics of the treated material. Indeed, remaining in the field of steel processing, hot rolling and cold rolling present significant differences, for instance in the controller structures, despite they could seem similar processes (see [1]).

The control tasks realized in the Level 1 automation of cold tandem mills mainly concern the thickness (gauge) (AGC – *automatic gauge control*) (see e.g. [6]) and the flatness (AFC –*automatic flatness control*) (see [7,8]). It is worthwhile to point out that both AGC and AFC rationales can change significantly from installation to installation, according to the mechanical solution considered and the sensors availability.

The flatness of the material can be defined as its ability to lie on a flat surface under gravity alone (see [9,10]). For a strip subject to cold rolling, the flatness can be more properly defined as the amount of internal stress difference along the width of the material. The measurement of the strip internal stresses (the so-called *shape*) during coiling can be taken through suitable sensors named *shapemeters* or *stressometers* that until now represent a significant investment. Due to the cost of these sensors only seldom a plant is equipped with more than one flatness sensor, i.e. the shapemeter installed at the exit of the mill.

Despite the cold tandem mill is constituted in general of several rolling stands with effective flatness actuators, the AFC task is usually performed by exploiting in closed-loop the flatness actuators of the last stand only, since it is the nearest to the shapemeter and it has the most immediate and predictable effect on the coil final flatness. In this paper an extension of the traditional AFC task is presented in order to exploit the compensation properties of other

* Corresponding author.
E-mail addresses: bemporad@dii.unisi.it (A. Bemporad), bernardini@dii.unisi.it (D. Bernardini), f.cuzzola@dca.it (F.A. Cuzzola), spinelli@dii.unisi.it (A. Spinelli).

0959-1524/$ - see front matter © 2010 Elsevier Ltd. All rights reserved.
doi:10.1016/j.jprocont.2010.02.003

stands, and three control techniques based on online optimization and delay compensation are proposed. Both a centralized control scheme, where a single controller computes the input signals for all the actuators, and a decentralized solution, where each stand of the mill is optimized locally to lower the computational burden, are investigated.

Including more than one stand in the control loop could lead to non-negligible advantages. For instance, for ultra-thin gauges (under 0.2 mm), the flatness at exit of some preliminary stands must be controlled, in order to avoid roll kissing in those stands where this phenomenon could potentially happen, so as to reduce the risk of cobbles and improve the final quality of both thickness and flatness.

As a benchmark example to evaluate the performance of the presented control approaches, we consider a cold tandem mill equipped by only one shapemeter and constituted of five stands, where the last one is of 6-high type. In this work, we will neglect the physical phenomena that can be observed in a *continuous* cold tandem mill (see e.g. [11]), i.e. a cold tandem mill coupled with a so-called *pickling line* used to eliminate the oxide scale from the surface of the black material coming from hot rolling process. However, results here presented can be easily extended in several directions to take into consideration other plant configurations.

The paper is organized as follows. Section 2 describes the physical structure of a 6-high rolling stand, whereas Section 3 is dedicated to the mathematical models used for flatness setup optimization. In Section 4 novel approaches for control of flatness based on quadratic optimization and delay compensation are presented. The performances of the proposed control schemes are illustrated by simulation results reported in Section 5, and conclusions are drawn in Section 6.

2. Structure of a 6-high stand

Each rolling stand of the mill is composed of a stack of rolls. For a 6-high mill the rolls are named respectively *work roll* – WR (i.e. the roll in contact with the material), *back-up roll* – BUR (the biggest roll at the top controlled by an hydraulic cylinder) and the *intermediate roll* – IR, placed in the middle between the work and the back-up roll (see Fig. 1). A 4-high stand has not the intermediate roll and consequently it has not the flatness actuators connected with it. Of course, a 6-high stand is expected to have the possibility to correct a wider set of flatness defects, because of the wider availability of flatness actuators.

Hereafter the flatness actuators which are available on a 6-high type stand are briefly described (see Fig. 2):

(1) The work roll bending (WRB). It allows applying a curvature on the work rolls. This actuator is fast but can reach saturation.
(2) Differential work roll bending (DWRB). The applied WRB can be different between the two sides of the stand (non-drive side/drive side).
(3) The intermediate roll bending (IRB). It is similar to the WRB, the difference is that it acts on the rolls placed in the middle of the roll stack.
(4) The work roll shifting (WRS). It has an influence on the flatness on the strip edges.
(5) The intermediate roll shifting (IRS). In case the intermediate rolls have a tapered-crown profile, its effect is similar to that of WRB and IRB.
(6) The intermediate roll crossing (IRC). The intermediate roll can be crossed with respect to the work rolls, producing a curvature of them.
(7) The tilting (T). It is the difference in gap between the two sides of the stand.
(8) Selective cooling (SC). The stand is provided of water nozzles distributed along the length of the work roll, in order to selectively cool parts of the work rolls.

Some of these flatness actuators can only be moved offline (i.e. before strip threading, at the setup generation) due to the direct contact with the material or to mechanical limitations. Among them, the WRS, as far as the authors know, has never been used in closed-loop in any installation. Indeed, it is in general used to control the thickness edge-drop (see e.g. [12]).

The other flatness actuators can be moved both offline (according to the material characteristics and the shape target) and in closed-loop during rolling (WRB, DWRB, IRB, IRC, T, SC). In particular, the IRC is an extremely powerful actuator which on the other hand presents a slow dynamical response. For this reason it is mainly used offline to compensate the thermal condition of the

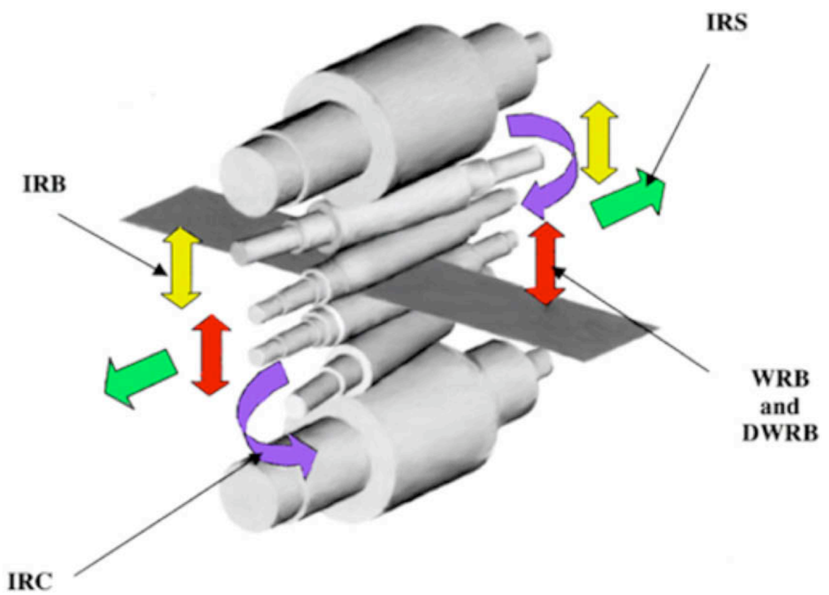

Fig. 1. A 6-high type stand for cold rolling.

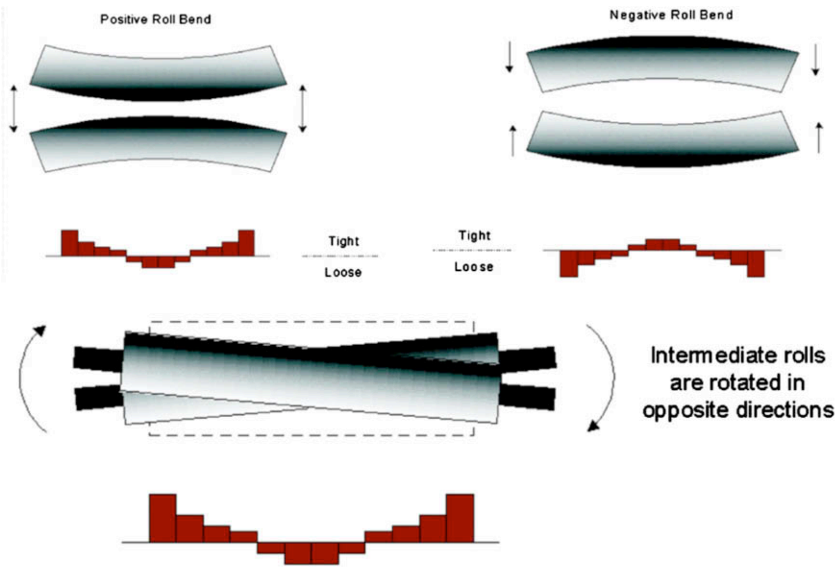

Fig. 2. Effects of bending and crossing on the shape.

plant during setup calculation, even if it can also be moved during rolling in order to recover from possible positive bending saturation (i.e. on WRB and/or IRB). The 4-high stands are not provided of the intermediate roll, and consequently only a subset of flatness actuators are available for them: WRB, DWRB, T, and SC.

In the following part of this paper a novel AFC technique is introduced, which allows to compensate measured flatness defects during rolling, on the basis of the measurements provided by a shapemeter.

In the AFC task of a tandem mill that will be discussed in the following these points need to be taken into account:

- Each actuator is subject to a dynamical response.
- The actuators commands are bounded. When a saturation limit is reached in a given stand, it is possible to use alternative flatness actuators in the same stand (for instance, IRC can be used to recover WRB/IRB from saturation), or to modify the configuration of other stands that are far from saturation in order to recover the saturation in the considered stand.
- Each stand presents a different transport delay from the shape sensor, since this is placed at the exit side of the tandem mill, i.e. after the last stand. These delays need to be suitably compensated in order to guarantee closed-loop stability (see Fig. 3).

3. The use of mathematical models for setup optimization

The automation system includes a supervision system (Level 2 automation). The main purpose of Level 2 automation is to supervise the plant and to compute a plant setup on the basis of the primary data of the product to be realized. It needs to include the following functions:

- The definition of the *shape targets* to be realized by each stand.
- The predicted optimal values for all the flatness actuators (in particular for the stands not optimized in closed-loop).
- The sensitivities on the coil shape of each flatness actuator for all the stands.

In order to achieve the optimal setup, the Level 2 system is equipped of several mathematical models (see also [2,3]):

- A *roll thermal crown model* (RTCM). This model simulates in a dynamical way the evolution of the thermal condition of the work rolls and, in particular, it allows to estimate the work roll profile variations due to thermal expansion (thermal crown). Typically this model is implemented in terms of a time-based integration of a power balance equation applied to the mass of the roll, and complemented with a *discrete element method* (DEM) based algorithm. The output of the model is represented by the thermal expansion profile of the roll.
- A *roll stack deflection model* (RSDM). It is a static model whose purpose is to evaluate the deflection of the rolls according to the rolling force and the roll thermal crown estimation provided by RTCM. Furthermore, it allows to estimate how the rolling pressure is distributed in the contact surfaces between rolls. This model can also be implemented through a DEM algorithm that allows to compute the distribution of the pressure in the contact surface.

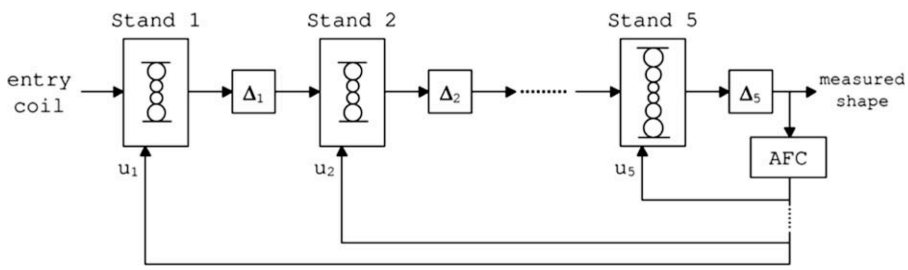

Fig. 3. Structure of a 5-stand tandem mill with 4-high stands, and a 6-high stand as last stand.

– The *shape model* (SM) is a static model that is in charge of estimating the strip internal stresses due to the pressure distribution in the contact surface between the WR and the material, given the estimated deflections provided by the RSDM. Besides, it provides an estimation of the material profile and, in particular, of the thickness edge-drop (i.e. the thickness variation at the strip edges with respect to the average value, see [12]) to be possibly compensated with a work roll shifting.

In general all the flatness models are exploited during setup computation but not during AFC closed-loop execution, due to the high involved computational complexity. The AFC task is in any case provided by a *linearized version* of these models, in order to implement additional predictive compensation effects. In the following, this linearized model will be referred to as "*sensitivity matrix*" or "*actuator influence matrix*". Of course, the sensitivity matrix generated in the setup computation is a representation of the shape phenomena in a given working point, hence that matrix needs to be recomputed coil-by-coil together with each plant setup.

The mentioned computational complexity of the shape models is not an issue for exploiting these models in an *offline simulation* of the complete AFC task, that can be used to evaluate the performance of the controller. For this reason, the simulations that will be presented in the following will take into account all the nonlinear phenomena predicted by means of these physical models.

As anticipated, one of the main contents of the setup is represented by the *shape targets* to be realized by each rolling stand. Each stand contributes through the shape control not only to the quality of the material but also to the stability of the mill.

The optimal flatness actuators configuration during setup calculation can be achieved by exploiting the shape estimations obtained from the SM (and the other flatness models, i.e. the RSDM and the RTCM) in a iterative algorithm whose purpose is to bring the SM shape estimation of every stand as near as possible to the corresponding shape target.

The Level 1 automation system implements the closed-loop control starting from the reference values generated by Level 2 and the feedback provided by the measurement system. As already pointed out, it is unlikely to have more than one shapemeter in a plant.

The following subsections are dedicated to the description of a shapemeter and the conventional implementation of the closed-loop AFC.

3.1. Shape measurement system

A conventional shapemeter used in cold rolling is constituted of an array of load cells distributed along the width of the strip. Each load cell produces a signal representing the pressure exercised by the slice of strip in contact with it. Consequently, the shapemeter produces an array of tension signals whose dimension is the number L of load cells placed on the sensor:

$$Shape = [T_1\ T_2\ \ldots\ T_L]'. \tag{1}$$

The presence of a gradient in the specific tensions associated to two different strip slices implies that the two slides will present different elongation values (see Fig. 4). In turn, a difference in the elongation between the strip slices could imply a flatness defect that should be corrected.

The shapemeter dynamics are extremely fast with respect to other dynamical effects such as the transport delay between the last stand and the exit shapemeter. For this reason, in the following part of the paper possible dynamics associated to the shapemeter will be neglected.

3.2. The conventional AFC system based on least mean squares

The problem of correcting a flatness defect, i.e. a deviation of the measured shape with respect to the desired shape target, can be properly faced if the influence of each flatness actuator on each tension measurement T_i is known, $i = 1, 2, \ldots, L$. In other words, it is necessary to know the relation

$$\begin{aligned}\Delta Shape(Act) &= [\Delta T_1(Act)\ DeltaT_2(Act)\ \ldots\ DeltaT_L(Act)]' \\ &= M(Act)DeltaAct\end{aligned} \tag{2}$$

for each actuator, where Act is a generic flatness actuator and $M(Act)$ is a vector of dimension L representing the *sensitivity matrix* of actuator Act on the shape. As reported before, the *sensitivity matrices* $M(Act)$ are computed by the Level 2 automation flatness models (SM, RSDM and RTCM).

Once the matrices $M(Act)$ are known, the closed-loop control problem is conventionally solved by means of *least mean squares* (LMS) (see Fig. 5). At each time instant the shape error, computed as the difference between the shape measurement and the shape target, is provided to an optimization tool based on LMS which computes the optimal variation of each actuator status with reference to their current status (see [13]). As discussed before, the IRC

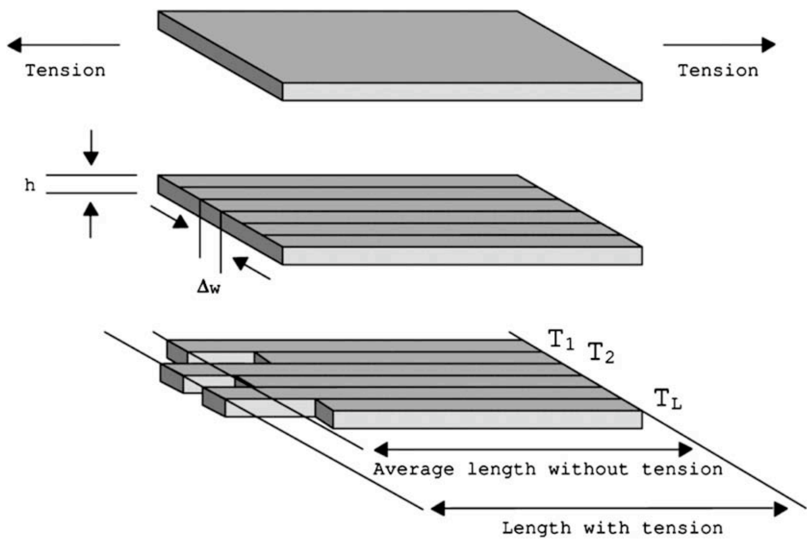

Fig. 4. The flatness defect is induced by differential internal tensions causing differential elongations.

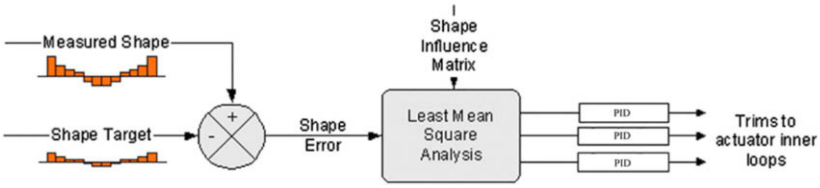

Fig. 5. AFC by means of least mean squares.

is a slow actuator and consequently its dynamics can be hardly neglected. For this reason the IRC control action cannot be computed by means of the just described LMS algorithm, and it is in general computed in cascade to the LMS algorithm in order to prevent saturation of WRB and/or IRB.

The use of LMS in the field is actually complemented of additional logic, often considered reserved *know-how*, that is in charge of avoiding several problems that LMS cannot solve by itself: as an example, it is necessary to execute the control algorithm even when two flatness actuators have similar yet not identical effects (sensitivities). In line of principle, in such a situation the bare LMS algorithm could produce as optimal result a flatness actuators configuration having some actuators uselessly fighting between them, or a configuration that cannot be actually implemented due to actuators saturation. Similar reasons motivate the adoption of model predictive control in order to explicitly take into account constraints without the use of additional logic.

In the rest of the paper three novel control algorithms based on online optimization are proposed, aiming to overcome the above issues.

4. Control algorithms

We start giving some preliminaries on model predictive control (MPC), a technology diffused in the general field of control of sheet and film processes, whose cold rolling mills control is an example [5].

MPC is widely spread in industry for control design of highly complex multivariable processes under constraints on input and state variables [14–16]. The idea behind MPC is to solve at each sampling time an open-loop finite-horizon optimal control problem based on a given prediction model of the process, by taking the current state of the process as the initial state. Only the first sample of the sequence of future optimal control moves is applied to the process. At the next time step, the remaining moves are discarded and a new optimal control problem based on new measurements is solved over a shifted prediction horizon. When the prediction model and the constraints are linear, and the control objective is expressed through a quadratic function, the computation of the control action requires the solution of a quadratic programming (QP) problem. An alternative approach to evaluate the MPC law was proposed in [17]: rather than solving the QP problem on line for the current state vector, by employing techniques of multiparametric QP the problem is solved offline for all state vectors within a given range, providing the *explicit* dependence of the control input on the state and reference, which is piecewise affine and continuous.

The straightforward application of the basic MPC algorithm to the whole tandem mill dynamical model is not viable because of the excessive computational burden involved (for instance, in [10] the authors implement an MPC scheme only on the last three stands of the mill and make assumptions on the strip structure to lower complexity). Neither the decentralized MPC approach recently proposed in literature (see [18–20]) is realizable, owing to the presence of delays between stands. Henceforth, relying on the model introduced below in Section 4.1, different solutions for control of tandem mills based on quadratic optimization and delay compensation are examined. The three alternative QP-based control schemes presented in the following will be referred to as Global QP controller (Section 4.2), Decentralized QP controller "*Optimize* & *Push*" (Section 4.3), Decentralized QP controller "*Pull* & *Optimize*" (Section 4.4).

4.1. Model of tandem mill for control

A single stand is modeled as the linear system depicted in Fig. 6, where

- $V \in \mathbb{R}^L$ is the input shape, where L is the number of zones the strip surface is divided.
- $Y \in \mathbb{R}^L$ is the output shape, corresponding to the input shape of the following stand.
- Δ is a transport delay, representing the strip rolling time from stand i to stand $i+1$ (or to the shapemeter, for the last stand) expressed as a number of sampling steps, where the sampling time is $T_s = 10$ ms. The delay of stand $\#i$ is denoted by $\Delta(i)$ and is assumed to be known during a specific coil rolling.
- $U_j \in \mathbb{R}$ is the actuation command input, $j = 1, \ldots, n$. The effect of actuator $\#j$ on Y is modeled through a sensitivity vector $M_j \in \mathbb{R}^L$, pre-calculated from Level 2 automation flatness models by linearization, and a first order dynamics

$$f(s) = \frac{1}{1 + \tau s} \tag{3}$$

with time constant $\tau = 0.1$ s. The choice of the dynamical model (3) can be reviewed according to the characteristics of the considered actuator, however, using a first order dynamics can be considered a fair approximation for hydraulically controlled actuators like WRB and IRB (see e.g. [13,21]). If a stand has more than one active actuator, the order of the actuators in the vector U is assumed to be the one listed in Section 2.
- RTC is the *roll thermal crown* disturbance input, modeled again as the cascade of a sensitivity vector and a first order dynamics.

The overall tandem mill model consists of the series cascade of the single stand models described above. In general, different stands are equipped with different combinations of active actuators. By letting n be the total number of actuators, the *global sensitivity matrix* $M \in \mathbb{R}^{L \times n}$ for the whole system model is defined by collecting the column sensitivity vectors from each stand. M maps statically the effect of each actuator on the output shape at the end of the tandem mill and takes into account the thickness reduction effects realized by each stand. This is measured through a shapemeter sensor placed at the exit of the last stand providing L values, one for each zone along the width of the strip.

As told, the assumption of having only one shapemeter after the last stand corresponds to the most common plant configuration, but the use of intermediate shapemeters could be considered and managed by the control techniques proposed hereafter.

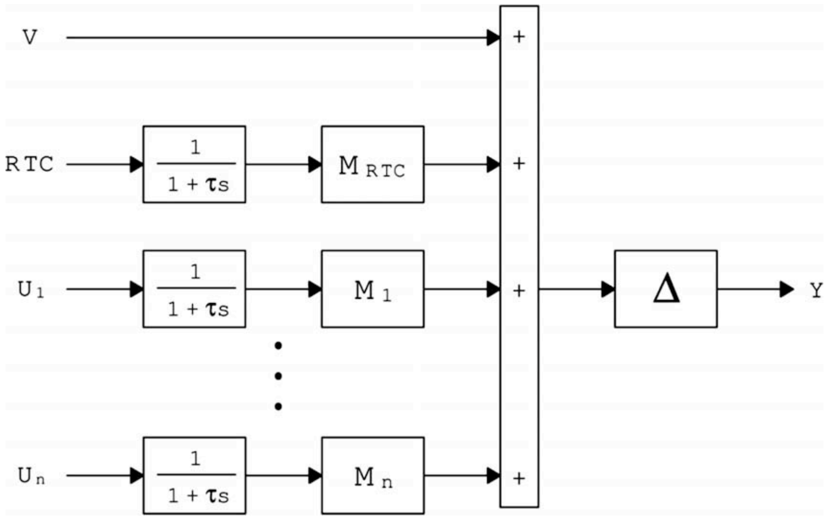

Fig. 6. Block diagram of one stand.

Since usually $L > n$, a common approach proposed in literature is to parameterize the shape profile in order to obtain M as a square matrix and simplify calculations [13,21,22,5]. In the following, we do not take into consideration strip parametrization explicitly, as it can be implemented independently of the specific control scheme adopted.

Since the linearized model of the tandem mill refers to a specific working point of the process, in presence of coil changes or substantial variations of coil properties such as speed, temperature or lubrication, the performances can degrade due to a non-optimal tuning of controller data M and Δ.

The re-calculation of Δ is trivial being the distance between stands fixed, whereas M is updated by Level 2 automation. More precisely the Level 2 automation models are provided also of complex auto-adaptation algorithms that exploit the measured feedback and are in charge of coil-by-coil automatically and recursively re-tuning the models exploited for computing M. This auto-adaptation task is executed online and will influence AFC only for the following coil, by modifying the "*actuator influence matrix*" M to be generated together with the setup (in general, it turns out counterproductive to perturb the AFC task for the current coil).

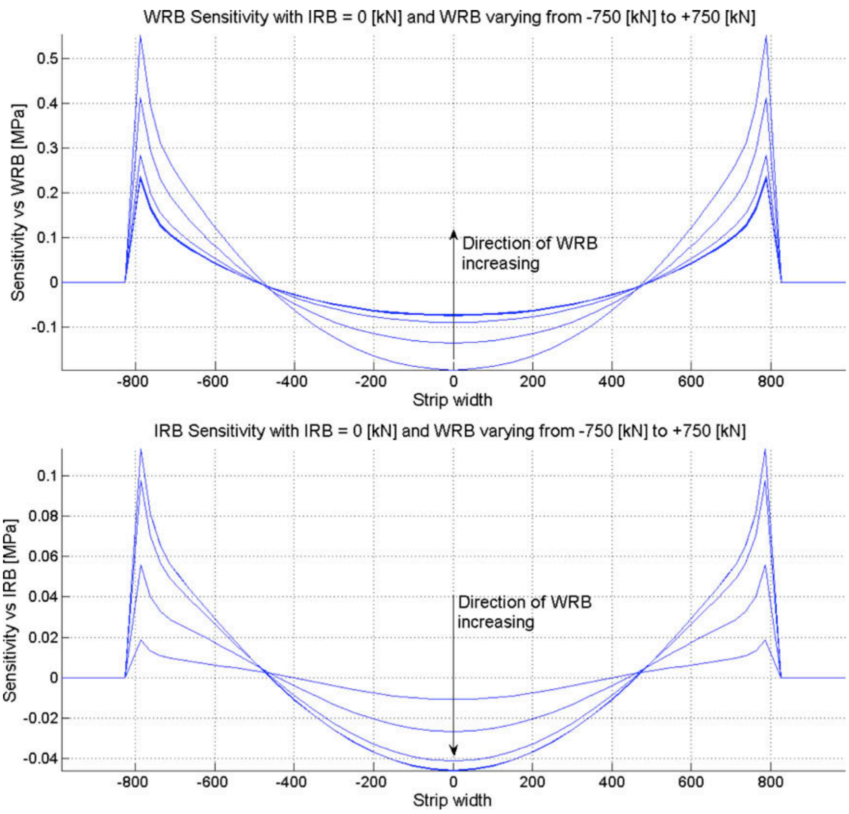

Fig. 7. Bending sensitivity variability in a 6-high mill.

In order to clarify the effects of the model uncertainties on the controller performances, it is worth concentrating on the variability of the parts of matrix M concerning WRB and IRB influence coefficients. As an example, Fig. 7 shows typical predicted influence coefficients for a strip of 1600 [mm] wide for a 6-high mill when the WRB is varying from −750 [kN] to +750 [kN]. As can be seen, the sensitivity coefficients are subject to significant variations despite the concave characteristic remains positive. In general, this effect leads to the practice that unreliable initial predictions of the setup produce inaccurate shape control actions, even though the stability is hardly compromised. Typically, in that case a poor shape regulation at the strip edges may occur, because the controller is not able anymore to discern between the effects of WRB and IRB.

4.2. Global QP controller

The Global QP control algorithm considers a single QP problem for the whole tandem mill (see Fig. 8). The idea is to have a central unit solving the following optimization problem at each time step k

$$\min_{U(k)} \ \|Y(k) - R(k) + M(U(k) - U_{old}(k))\|_2^2 \tag{4a}$$

$$\text{s.t.} \quad U_{\min} \leqslant U(k) \leqslant U_{\max} \tag{4b}$$

involving the overall delay-free model of the tandem mill composed of N stands, where:

- $Y(k) \in \mathbb{R}^L$ is the vector of output zones measured at the end of the tandem mill.
- $R(k) \in \mathbb{R}^L$ is the set point for Y.
- $U(k) \in \mathbb{R}^n$ is the vector collecting all actuator values.
- $U_{old}(k)$ is the filtered version of the vector of previous actuator values $U(k - \sum_{i=1}^{N}\Delta(i))$ that contributed to generate the output $Y(k)$ at the current time k. The filtering is obtained through the first order dynamics (3), in order to consider the actual (low-pass filtered) values applied by actuators.
- $U_{\min}$ and $U_{\max}$ are lower and upper bounds for the control signal $U(k)$, respectively. Constraint (4b) is intended in a component-wise fashion.

In order to take into account the relevant delays in the system, a *Synchronizer* block supplies each actuation command at the right time. Once the input for stand $\#i$ has been calculated, it is placed into a buffer with a delay $\Delta_{buf}(i)$, such that

$$\Delta_{buf}(i) = \sum_{j=1}^{i-1} \Delta(j), \quad i = 1, \ldots, N. \tag{5}$$

The drawback of the Global QP control approach is the amount of computations involved in solving the centralized problem (4), especially when a large number of stands and actuators is involved. Decentralized, computationally lighter approaches are therefore explored in the next sections.

4.3. Decentralized QP controller “Optimize & Push”

The first solution consists of a simpler QP controller placed at every stand, working in parallel with the others. The principle is the same as the global one because every single QP optimizes a delay-free system and send its data to the Synchronizer (see Fig. 9). As no information exchange among QP controllers happens during the decentralized computation at time k, every QP controller operates under the assumption that at time k the other QP controllers maintain applied their values, which have been previously calculated at time $k-1$, therefore leading to sub-optimal solutions. For a generic stand $\#i$ at time step k the optimization problem to be solved is

$$\min_{U_v(k)} \ \|Y(k) - (R(k) - M_c U_{prev}(k)) + M_v U_v(k) - M U_{old}(k)\|_2^2 \tag{6a}$$

$$\text{s.t.} \quad U_{v,\min} \leqslant U_v(k) \leqslant U_{v,\max} \tag{6b}$$

where $Y,\ R,\ U_{old}$ are defined as in (4), and

- M_v is the sensitivity matrix of stand $\#i$ composed by extracting the column vectors of the global sensitivity matrix M corresponding to the actuators that are actively used at that stand.
- M_c is the complement of M_v, related to actuators that are not optimized at stand $\#i$, ordered by stand number, from the input shape to the shapemeter.
- $U_v(k)$ are the actuators values for stand $\#i$.
- $U_{prev}(k)$ is the filtered version through (3) of the actuators signals optimized at the other stands and computed at the previous time step $k-1$.
- $U_{v,\min},\ U_{v,\max}$ are respectively the elements of $U_{\min},\ U_{\max}$ referred to the actuators optimized by stand $\#i$.

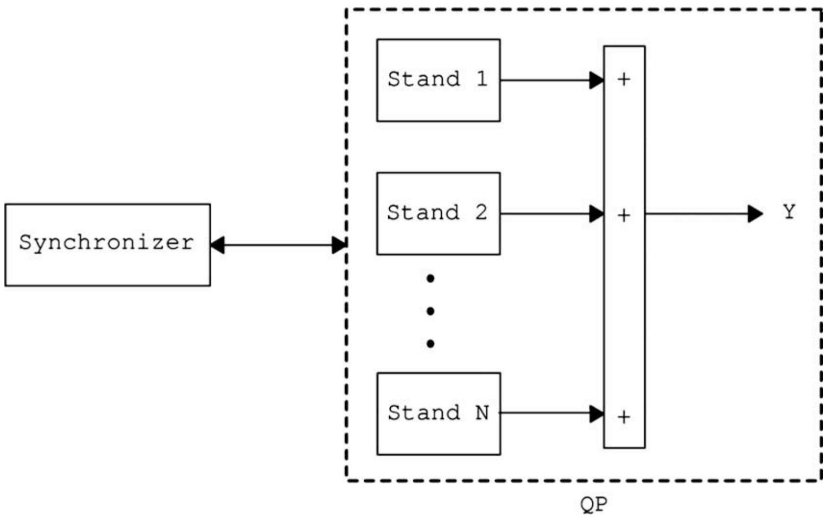

Fig. 8. Virtual delay-free model for Global QP controller.

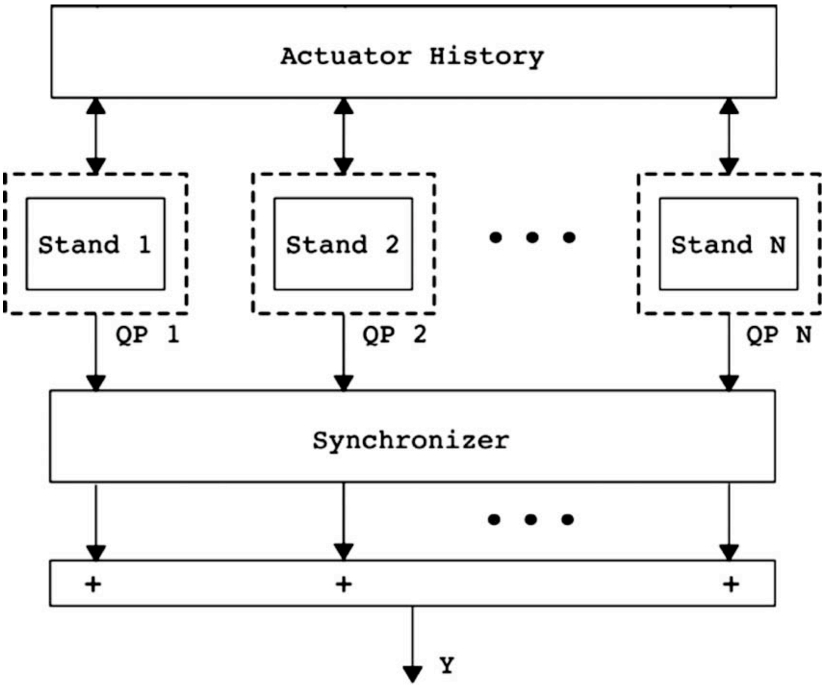

Fig. 9. Virtual delay-free model for Decentralized QP controller "Optimize & Push".

Note that, while communication among stands takes place to obtain U_{prev}, no exchange of information happens during the optimization of each stand.

A variation of the above scheme leading to an improved overall closed-loop response consists of including the dynamics (3) of the WRB actuator in the optimization of the first stand. This is achieved by considering the input values obtained from the static QP minimization as set-points to an explicit MPC controller based on the actuator dynamics (3) of the first stand.

The MPC problem is formulated using the model predictive control toolbox [23] as:

$$\min_{\Delta U_1} \sum_{j=0}^{p-1} \|y(k+j|k) - U_1^{qp}\|_2^2 \tag{7a}$$

$$\text{s.t.} \quad y(k+j+1|k) = e^{-T_s/\tau} y(k+j|k) + (1 - e^{-T_s/\tau}) u(k+j|k), \tag{7b}$$

$$u(k+j+1|k) = u(k+j|k) + \Delta u(k+j|k), \tag{7c}$$

$$U_{1,\min} \leqslant u(k+j|k) \leqslant U_{1,\max}, \quad \forall j = 0, \ldots, m-1, \tag{7d}$$

$$\Delta u(k+j|k) = 0, \quad \forall j = m, \ldots, p, \tag{7e}$$

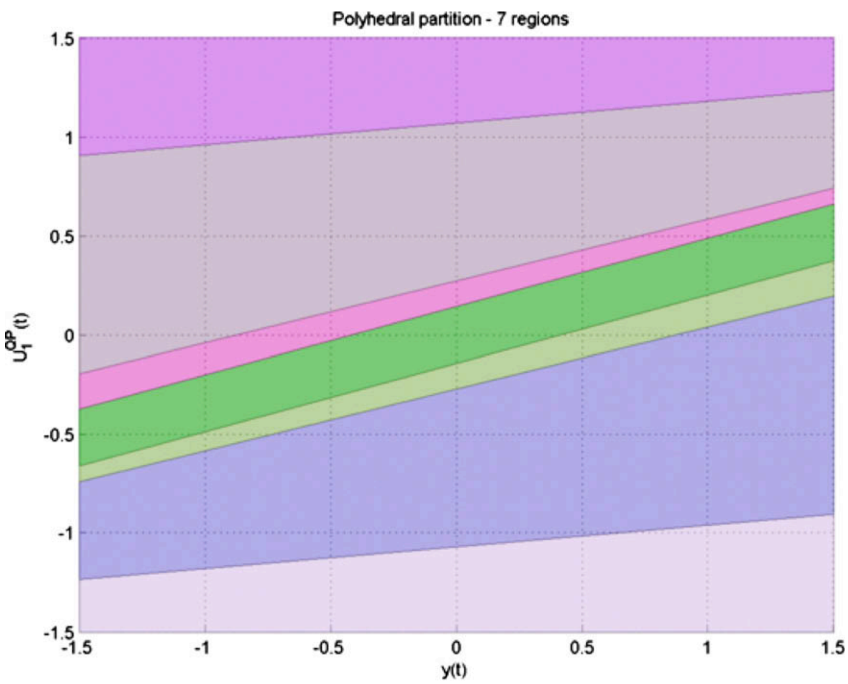

Fig. 10. Explicit MPC controller (7e). Section of the controller partition in the $(y(k), U_1^{qp}(k))$-space obtained for $u(k-1) = 0$.

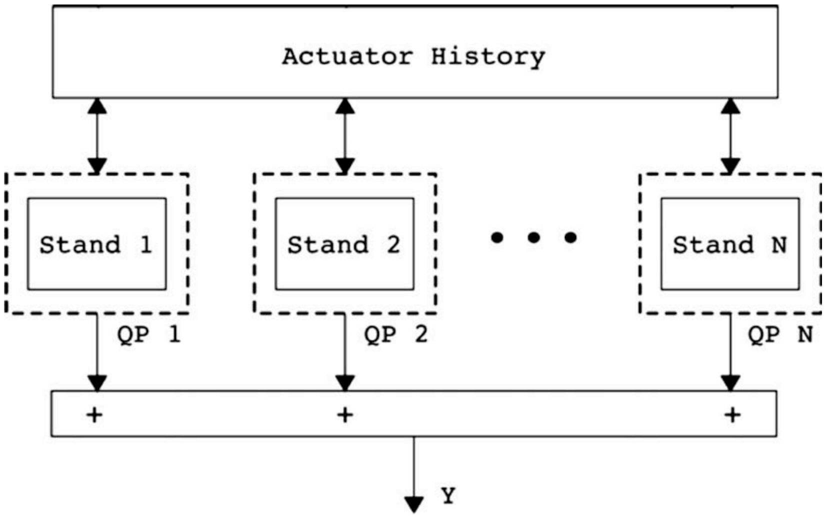

Fig. 11. Virtual model for Decentralized QP controller "Pull & Optimize".

where $y(k+j|k) \in \mathbb{R}$ is the output of the WRB actuator at prediction time $k+j$ obtained by sampling dynamics (3), $u(k+j|k) \in \mathbb{R}$ and $\Delta u(k+j|k) \in \mathbb{R}$ are the predicted command to the actuator and its finite difference, respectively, $\Delta U_1 = \{\Delta u(k|k), \ldots, \Delta u(k+m-1|k)\}$, and U_1^{qp} is the input value commanded to WRB by the first stand QP. The prediction horizon $p = 20$ and the control horizon $m = 3$ have been tuned to achieve a desirable trade-off between closed-loop performance and involved computational load. The MPC controller is converted to its explicit form by using the hybrid toolbox [24], resulting in a piecewise affine control law depicted in Fig. 10, defined over 7 polyhedral partitions of the $(y(k), u(k-1), U_1^{qp}(k))$-space (see Fig. 10).

As no sensor is available to measure the actual command $y(k)$ delivered at each time step k by the WRB actuator, the above MPC controller works purely in feedforward, having the effect of filtering the WRB command U_1^{qp} by taking into account the actuator dynamics (3) and its upper and lower bounds.

Note that adding an (explicit) MPC control action on all stands has the negative consequence of requiring a global coordination among all MPC controllers, which is avoided here in order to maintain the computational simplicity of the decentralized scheme.

4.4. Decentralized QP controller "Pull & Optimize"

A rather different control approach that still maintains the desired low computational effort of the Decentralized QP solution presented above consists of getting rid of the global Synchronize block. After an input vector computed by a QP is calculated, it is applied to the stand without buffering. The basic idea is to formulate the optimization problems so that the ith QP is responsible to compute the command inputs to be actuated with no delay, considering the effects that other stands have had or will have on the *same section* of the strip which is currently being processed at the ith stand. Hence, a global delay-free model is no more employed (see Fig. 11).

As a consequence, the optimization of a generic stand $\#i$ at time k only requires the information about what the QPs at the previous stands $1, \ldots, i-1$ have applied on its current strip section in the past (which in general is different from the actuators values at the previous time step $k-1$), and a prediction of what the following stands $i+1, \ldots, N$ will apply on it. Accordingly, the problem solved at stand $\#i$ at time k is

$$\min_{U_v(k)} \|Y(k) - (R(k) - M_c U_{prev}^i(k)) + M_v U_v(k) - M U_{old}(k)\|_2^2 \tag{8a}$$

$$\text{s.t.} \quad U_{v,\min} \leqslant U_v(k) \leqslant U_{v,\max} \tag{8b}$$

where now $U_{prev}(k)$ is defined as $U_{prev}(k) = [U_{prev}^1 \; U_{prev}^2 \ldots \; U_{prev}^N]$,

$$U_{prev}^i(k) = \begin{vmatrix} U_1(k - \sum_{j=1}^{i-1} \Delta(j)) \\ U_2(k - \sum_{j=2}^{i-1} \Delta(j)) \\ \vdots \\ U_{i-1}(k - \Delta(i-1)) \\ U_{i+1}(k-1) \\ U_{i+2}(k-1) \\ \vdots \\ U_N(k-1) \end{vmatrix}, \tag{9}$$

U_j is the input vector computed for stand $\#j$, and the values $U_j(k-1)$, $j = i+1, \ldots, N$, are determined at time step $k-1$ as in the "Optimize & Push" scheme.

In principle, as for the "Optimize & Push" approach, an explicit MPC controller could be added for generating the actual actuator signals from the input values computed by the QP. However, in this case the first components $U_1(k - \sum_{j=1}^{i-1} \Delta(j))$ of U_{prev}^i in (9) would contain the values generated by the MPC controller. During the transient, such values may be wildly oscillating from one step to another. In the static optimization (8b) they are treated as steady-state values, a certainly wrong assumption during such transients. Henceforth, in this control scheme we will not include an MPC action on the first stand. Similarly, the MPC action on the first stand is not conveniently applicable in the Global QP control approach, as filtering the input values generated by the Global QP to stand $\#1$ through an MPC feedback loop would make the whole coordinated scheme clash. Note that, instead, in the "Optimize & Push" approach U_{prev}^i contains signals computed at the previous time step $k-1$, so that old transient values generated by the MPC controller at the first stand disappear immediately after they have been issued (even after one step if the filter (3) were not applied).

5. Numerical results

The control algorithms described in the previous section have been tested on a nonlinear simulator exploiting the same flatness models used in a real automation system (i.e. SM, RTCM, and RSDM), with $N = 5$ stands and the following actuators configuration: stands 1–4 are of 4-high type and are equipped with WRB only, while the 5th stand is of 6-high type and it is equipped with WRB, IRB and IRC. The resulting delay vector is given by $\Delta = [15, 11, 9, 7, 6]$. The strip shape is desired to assume the constant profile with zero mean shown in Fig. 12. The nonlinear simulation model includes the roll thermal crown dynamics, which affect the work rolls on all the stands of the mill. This disturbance is due to the thermal expansion of the rolls, which heat up during the rolling process, and produces an increased roll bending action. An example of thermal crown effects is illustrated in Fig. 13. To take into account other disturbances than roll thermal crown, the unmeasured disturbance

$$d(k) = \begin{cases} 0 & \text{if} \quad k < 2\,\text{s} \\ R/2 & \text{if} \quad k \geqslant 2\,\text{s} \end{cases} \tag{10}$$

is added on the output signal in the simulation model. This type of disturbance can be considered as a material sudden variation during weld transition in a continuous tandem rolling mill.

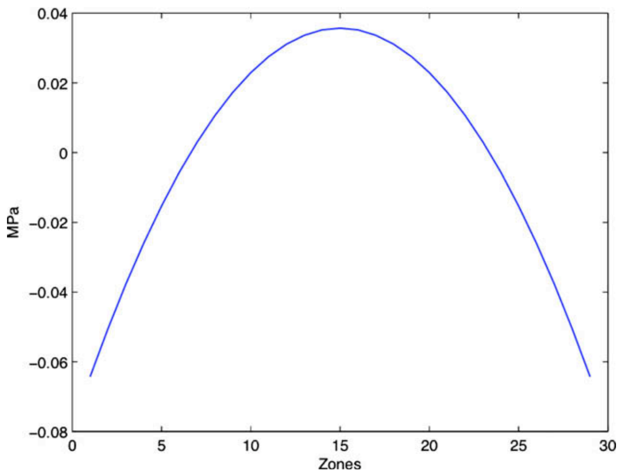

Fig. 12. Target strip shape R used in simulation.

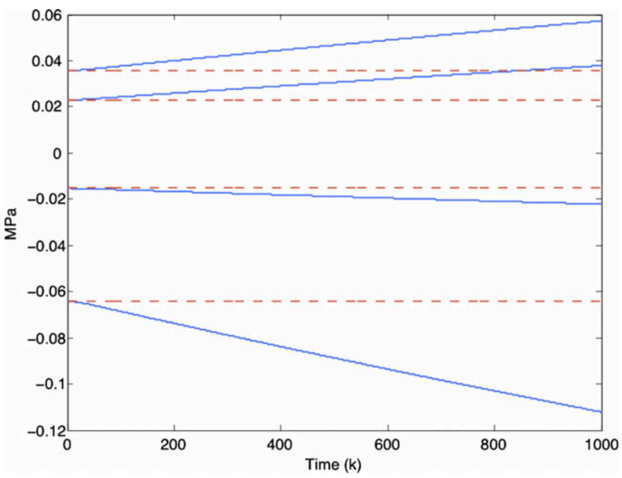

Fig. 13. Open-loop evolution of output shape of zones 1, 15, 20 and 25 due to roll thermal crown only (solid line), with respect to a given initial condition (dashed line).

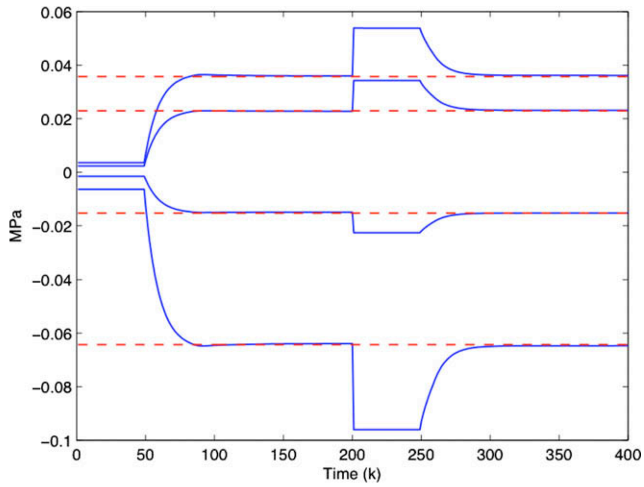

Fig. 14. Global QP control action, output shape of zones 1, 15, 20 and 25. Solid line: output, dashed line: target.

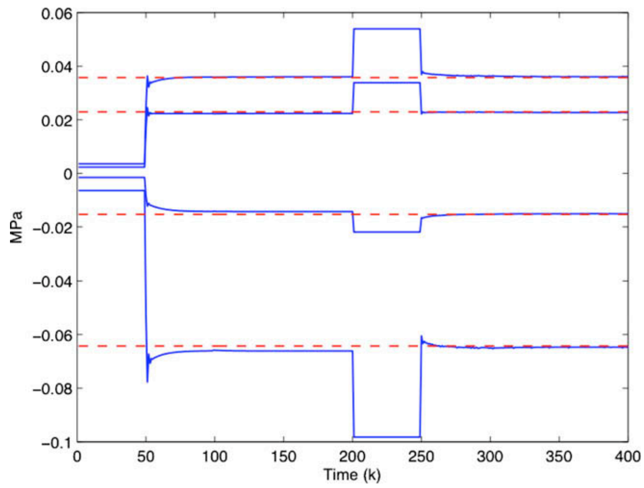

Fig. 15. Decentralized QP "Optimize & Push" control action, output shape of zones 1, 15, 20 and 25. Solid line: output, dashed line: target.

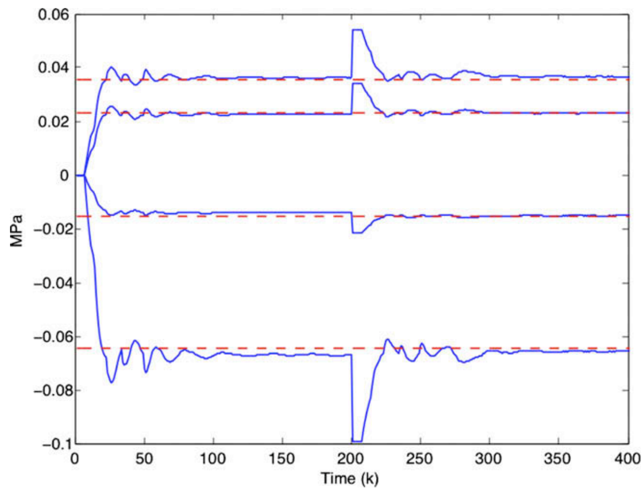

Fig. 16. Decentralized QP "Pull & Optimize" control action, output shape of zones 1, 15, 20 and 25. Solid line: output, dashed line: target.

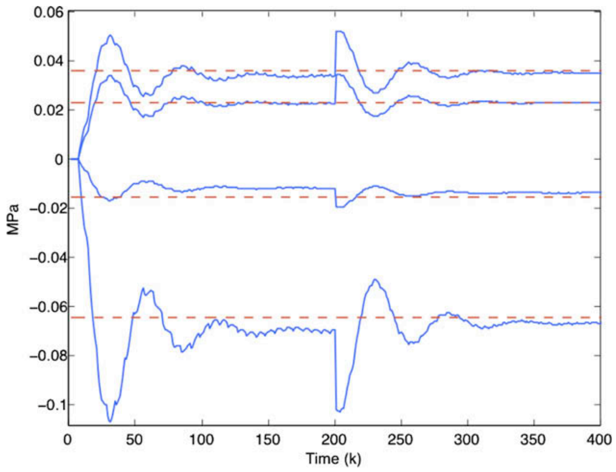

Fig. 17. LMS-based control action, output shape of zones 1, 15, 20 and 25. Solid line: output, dashed line: target.

Both the Global QP and the Decentralized QP "Optimize & Push" + MPC approaches, whose performances are, respectively, depicted in Figs. 14 and 15, show a smooth behavior with no output oscillations, thanks to the coordinated action between stands. Their delayed reaction to the disturbance is due to the delay-free model employed for the static QP optimization. The decentralized solution shows a much better rising time with respect to the global control thanks to the MPC action, which exploits partial knowledge of the process dynamics.

On the other hand, the Decentralized QP "Pull & Optimize" exhibits a faster reaction to the disturbance, see Fig. 16. The independence of the stands let them react more promptly to the disturbance. Such an increased autonomy is paid in terms of larger settling time and higher output oscillations, due to local models mismatches.

Moreover, we compared the proposed control schemes with a traditional LMS-based controller where only the WRB and IRB actuators equipped on the last stand are optimized online, and where no information on the actuator dynamics is exploited. In other words, at time k the LMS input command is obtained by the solution of problem (8b) for stand #5, where the variable corresponding to the IRC actuator is fixed to an optimal value computed offline (as well as the commands of all the actuators equipped on the stands #1 to #4), and no filtering through (3) is used to compute $U_{old}(k)$. Closed-loop behavior of this control approach is shown in Fig. 17. Table 1 reports comparative numerical results for $T_{sim} = 1000$ simulation steps, where performances have been evaluated using the cumulated norm of the tracking error as a benchmark, defined as $J = \sum_{k=1}^{T_{sim}} \|R - Y(k)\|_2$.

Table 1
Simulation results.

Controller	Perf. index J
LMS-based controller	17.89
Global QP controller	16.35
Decentralized QP "Optimize & Push"	16.59
Decentralized QP "Pull & Optimize"	8.39

Finally, Fig. 18 compares some significant input trajectories for the three proposed control techniques. The allowed minimum and maximum values for the showed actuators signals are −1.5 kN and 1.5 kN, respectively. The sub-optimality of the decentralized schemes with respect to the global controller is observable from the different steady-state input levels. Also, it is possible to see how MPC drives the controlled WRB actuator to saturation for short time intervals, in order to achieve fast reference tracking.

From a computational point of view, for the considered process setup the Global QP optimizes 7 variables subject to 14 constraints, while the Decentralized QPs optimize only 1 variable (3 for the last stand) subject to 2 constraints (6 for the last stand).

Of course, the simulations just presented can lead to degraded performance in presence of strong model uncertainties i.e. in case

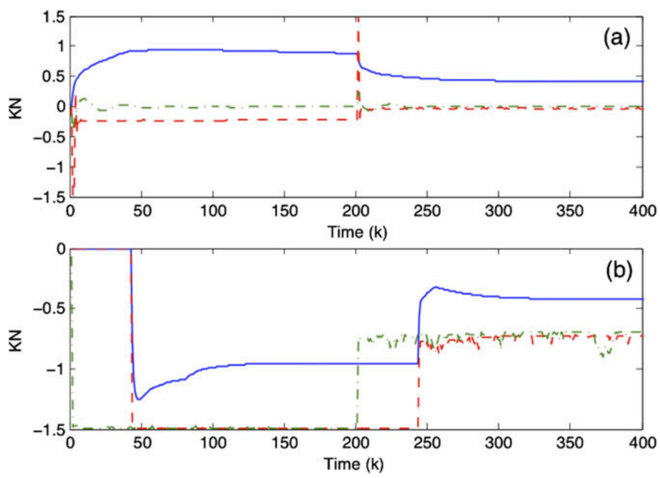

Fig. 18. Input signals of (a) WRB on stand #1, (b) IRB on stand #5, for Global QP (solid line), Decentralized QP "Optimize & Push" (dashed line), and Decentralized QP "Pull & Optimize" (dash-dotted line).

the steady-state tuning condition associated to the flatness model auto-adaptation algorithm has not been fully achieved. This performance degradation in such a case affects all the control algorithms considered and the performance classification presented in Table 1 does not change.

6. Conclusions

This paper has proposed three different control techniques based on quadratic optimization and delay compensation for control of flatness in cold tandem mills. Despite the fact that the process is multivariable, constrained and has numerous delays, all three approaches provide good closed-loop performance with limited computation requirements. In particular the decentralized solutions proposed in the paper present a computational complexity which is linearly increasing with the number of stands. The promising closed-loop performance obtained in simulation on a nonlinear mill model from one hand, and the limited software complexity for implementation on the other, provide significant encouragement for proceeding on the experimental validation of the design.

References

[1] W. Roberts, Flat Processing of Steel, Marcel Dekker, New York, NY, 1988.
[2] R. Guo, Optimal profile and shape control of flat sheet metal using multiple control devices, IEEE Transactions on Industry Applications 32 (1996) 449–457.
[3] R. Guo, Development of an optimal crown/shape level-2 control model for rolling mills with multiple control devices, IEEE Transaction on Control Systems Technology 6 (1998) 172–179.
[4] R. Guo, A. Malik, Development of a new crown/shape control model for cluster mills, Iron and Steel Technology 2 (2005) 31–42.
[5] J.V. Antwerp, A. Featherstone, R. Braatz, B. Ogunnaike, Cross-directional control of sheet and film processes, Automatica 43 (2007) 191–211.
[6] J. Pittner, M.A. Simaan, Optimal control of tandem cold rolling using a pointwise linear quadratic technique with trims, ASME Journal of Dynamic Systems Measurements and Control 130 (2) (2008) 021006-1–021006-11.
[7] T. Saito, T. Ohnishi, T. Komatsu, S. Miyoshi, H. Kitamura, M. Kitahama, Automatic flatness control in tandem cold rolling mill for ultra-thin gauge strip, Kawasaki Steel Technical Report 24 (1991) 41–46.
[8] S. Duncan, J. Allwood, S. Garimella, The analysis and design of spatial control systems in strip metal rolling, IEEE Transaction On Control System Technology 6 (1998) 220–232.
[9] D. Greenwood, G. Hearns, M. Grimble, M. Johnson, Co-ordinated hot strip mill load balancing, in: Proceedings of UKACC Control Conference, Cambridge, UK, 2000.
[10] B. Bulut, M. Katebi, M. Grimble, Co-ordinated control of profile and shape in hot strip finishing mills with nonlinear dynamics, Control Theory and Applications, IEE Proceedings 149 (2002) 471–480.
[11] J. Pittner, N. Samaras, M. Simaan, A novel approach for optimal control of continuous tandem cold metal rolling, in: Proceedings of the IEEE Industry Applications Society Annual Meeting, New Orleans, LA, 2007.
[12] K. Kitamura, T. Nakanishi, I. Yarita, N. Suganuma, K. Toyoshima, Edge-drop control of hot and cold rolled strip tapered-crown work roll shifting mill, Iron and Steel Engineer (1995) 27–32.
[13] M. Grimble, J. Fotakis, The design of strip shape control systems for Sendzimir mills, IEEE Transactions on Automatic Control 27 (1982) 656–666.
[14] J. Rawlings, Tutorial overview of model predictive control, IEEE Control Systems Magazine (2000) 38–52.
[15] E. Camacho, C. Bordons, Model predictive control, second ed., Advanced Textbooks in Control and Signal Processing, Springer-Verlag, London, UK, 2004.
[16] J. Maciejowski, Predictive Control with Constraints, Prentice Hall, Harlow, UK, 2002.
[17] A. Bemporad, M. Morari, V. Dua, E. Pistikopoulos, The explicit linear quadratic regulator for constrained systems, Automatica 38 (1) (2002) 3–20.
[18] A. Venkat, J. Rawlings, S. Wright, A framework for integrating model predictive controllers to control of large-scale systems, in: Annual AIChE Meeting, Cincinnati, OH, 2005.
[19] T. Keviczky, F. Borrelli, G. Balas, Decentralized receding horizon control for large scale dynamically decoupled systems, Automatica 42 (2006) 2105–2115.
[20] A. Alessio, A. Bemporad, Decentralized model predictive control of constrained linear systems, in: Proceedings of the European Control Conference, Kos, Greece, 2007, pp. 2813–2818.
[21] J. Ringwood, M. Grimble, Shape control in Sendzimir mills using both crown and intermediate roll actuators, IEEE Transactions on Automatic Control 35 (1990) 453–459.
[22] J. Ringwood, Shape control systems for Sendzimir steel mills, IEEE Control Systems Magazine 8 (2000) 70–86.
[23] A. Bemporad, M. Morari, N.L. Ricker, Model Predictive Control Toolbox for Matlab User's Guide, The Mathworks, Inc., 2004, http://www.mathworks.com/access/helpdesk/help/toolbox/mpc/.
[24] A. Bemporad, Hybrid Toolbox – User's Guide, 2004, http://www.dii.unisi.it/hybrid/toolbox.